

Supplementary Materials for

The Crystal Structure of a Self-Activating G Protein α Subunit Reveals Its Distinct Mechanism of Signal Initiation

Janice C. Jones, Jeffrey W. Duffy, Mischa Machius, Brenda R. S. Temple, Henrik G. Dohlman,* Alan M. Jones

*To whom correspondence should be addressed. E-mail: hdohlman@med.unc.edu

Published 8 February 2011, *Sci. Signal.* **4**, ra8 (2011)

DOI: 10.1126/scisignal.2001446

This PDF file includes:

Methods

Fig. S1. Solvent accessibility of guanine nucleotides in plant and animal G protein α subunits.

Fig. S2. *B* value analysis of AtGPA1.

Fig. S3. Nucleotide exchange by G protein α subunits.

Fig. S4. CD spectra of GDP-bound G protein α subunits.

Table S1. Data collection and refinement statistics for AtGPA1.

Table S2. GTP-binding rates for wild-type and mutant G protein α subunits.

Movie S1 legend.

Other Supplementary Material for this manuscript includes the following:

(available at www.sciencesignaling.org/cgi/content/full/4/159/ra8/DC1)

Table S3 (Microsoft Excel format). *B* value analysis of crystal structures of G protein α subunits.

Movie S1 (.avi format). Movie depicting domain motion in AtGPA1 generated from MD simulations.

Methods

Fluorescence-based measurement of the release of MANT-GMPPNP

Purified G protein α -subunit (400 nM) was added to a cuvette containing 1 ml of TEMNG buffer containing MANT-GMPPNP (400 nM, Jena Bioscience). The binding of MANT-GMPPNP was monitored by measuring the change in MANT fluorescence (excitation at 360 nm, emission at 440 nm). Once maximal binding was reached, GTP γ S (2 μ M) was added to compete with MANT-GMPPNP, and the resulting reduction in MANT fluorescence was monitored. The rate of release of MANT-GMPPNP was determined by fitting a one-phase, exponential decay curve with GraphPad Prism software.

Measurement of GTP binding by radionucleotide-binding assay

Purified G protein α -subunit (1 μ M) in HEL buffer [50 mM Hepes (pH 7.0), 1 mM EDTA, 0.1% (w/v) Lubrol, 1 mM DTT] was mixed with an equal volume of [35 S]GTP γ S buffer (HEL containing 10 mM MgCl₂, 5 μ M GTP γ S, and [35 S]GTP γ S at about 3,000 cpm/pmol) to start the binding reaction. At a given time point, duplicate 100- μ l aliquots from the reaction were quenched in 3 ml of ice-cold WB [20 mM Tris-HCl (pH 7.4), 100 mM NaCl, 25 mM MgCl₂] and immediately vacuum-filtered through nitrocellulose. Filters were quickly washed once with 3 ml of ice-cold WB, and total 35 S bound to the filter was quantified by scintillation counting.

Information on the measurement of protein stability by CD spectroscopy

The comparatively weak electron density in areas in the helical domain of our crystals of AtGPA1 indicated a pronounced intrinsic flexibility of its helical domain. In contrast, crystal structures of animal G protein α -subunits do not indicate an increased flexibility in the helical domain compared to that of the Ras domain (table S3). We investigated protein stability with CD spectroscopy by monitoring changes in secondary structure as a function of temperature. The CD spectra of the wild-type and chimeric proteins were similar, indicating comparable secondary structure content. The temperature-induced denaturation curve for G α_{i1} showed a steep transition, indicative of a highly cooperative unfolding process, with a midpoint of unfolding (“melting temperature”) of \sim 57°C (Fig. 3B). In contrast to G α_{i1} , the unfolding of AtGPA1 was much less cooperative. Indeed, the appearance of the denaturation curve indicates the presence of two kinetically distinct transitions, one below and one above 50°C. The thermal denaturation profile of AtGPA1^{i1Hel} was similar to that of G α_{i1} , with highly cooperative unfolding and a melting temperature of 62°C. Thus, replacing the helical domain of AtGPA1 with that of G α_{i1} rendered the AtGPA1^{i1Hel} chimera as stable as G α_{i1} . Conversely, replacing the helical domain of G α_{i1} with that of AtGPA1 conferred instability on G α_{i1} ^{AtHel}. These experiments showed that the nature of the helical domain strongly influences the unfolding properties of the G protein α -subunit.

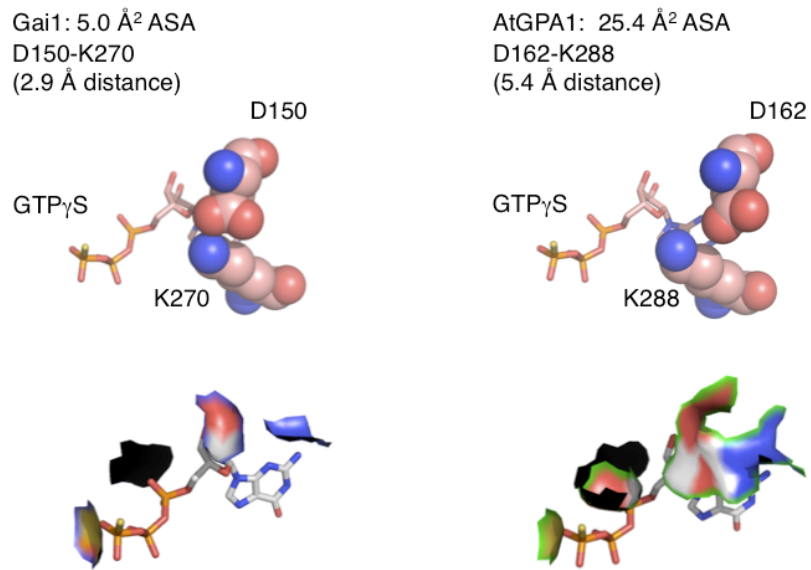


Fig. S1. Solvent accessibility of guanine nucleotides in plant and animal G protein α subunits. Space-fill models of residues at the interface between the helical and Ras domains of the indicated G protein α subunits (top structures). The surface map of solvent accessibility of GTP γ S (bottom structures) is increased in AtGPA1 relative to that of G α_{i1} because of reduced interdomain interactions.

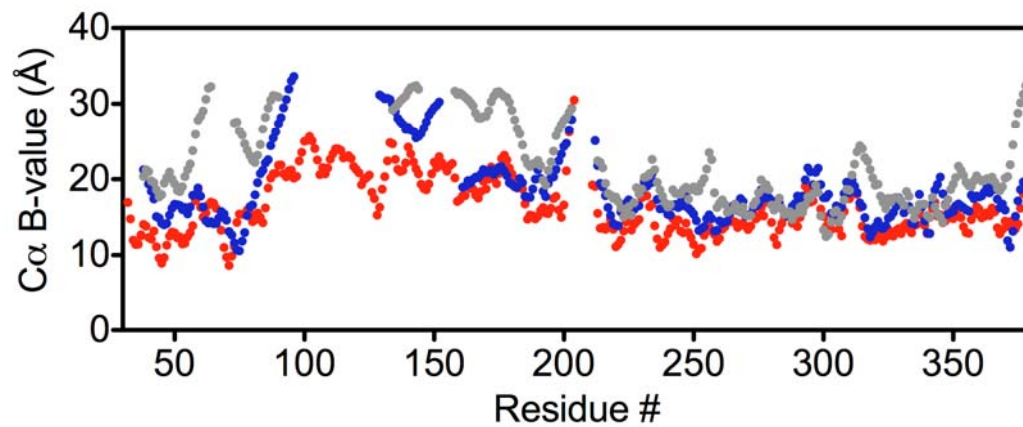


Fig. S2. *B* value analysis of AtGPA1. Atomic displacement parameters (“*B* values”) for each C α in monomers A (red), B (blue), and C (gray) of AtGPA1 are shown.

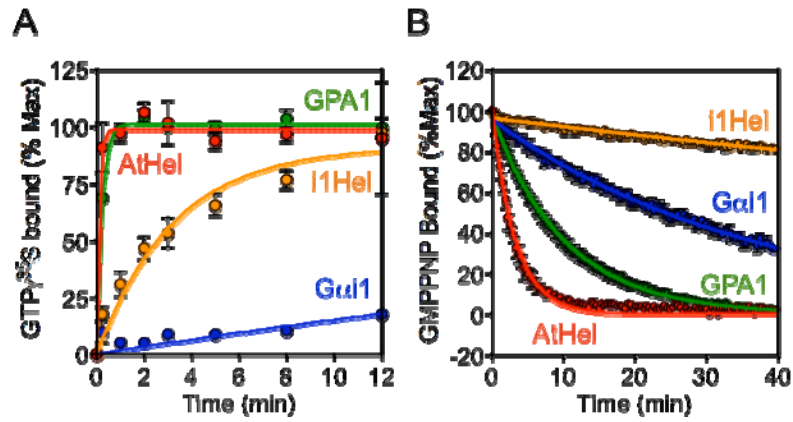


Fig. S3. Nucleotide exchange by G protein α subunits. **(A)** Radionucleotide-binding experiment. Purified His-tagged G protein α subunit (500 nM) was incubated with GTP γ ³⁵S (2 μ M) for the indicated time before samples were filtered through nitrocellulose and bound GTP γ ³⁵S was quantified. Data shown are the average \pm SEM for two experiments. **(B)** Fluorescence-based assay to measure the release of bound MANT-GMPPNP. G protein α subunit (400 nM) was loaded with MANT-GMPPNP (400 nM) before GTP γ S (2 μ M) was added at time 0. Data shown are the average \pm SEM for two experiments.

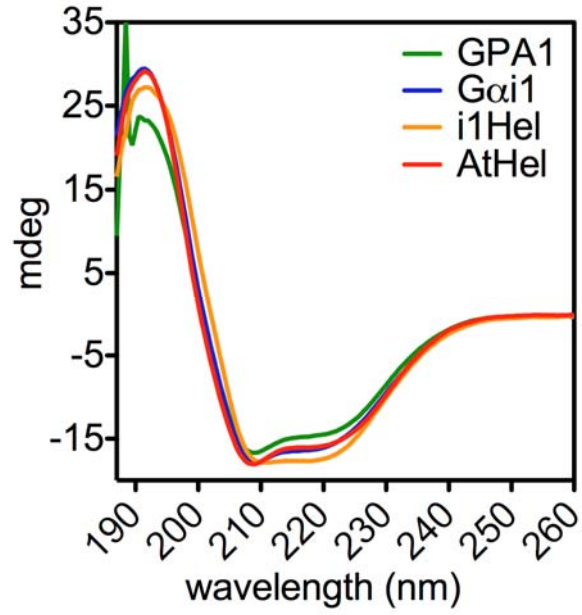


Fig. S4. CD spectra of GDP-bound G protein α subunits. Data were collected for the indicated G protein α subunits at 15°C, as described in the Materials and Methods (main text). mdeg, millidegrees. Data are representative of two experiments.

Table S1. Data collection and refinement statistics for AtGPA1.

AtGPA1	
Data collection	
Space group	P2 ₁ 2 ₁ 2 ₁
Cell dimensions	
<i>a</i> , <i>b</i> , <i>c</i> (Å)	67.13, 119.35, 161.73
α , β , γ (°)	90, 90, 90
Resolution (Å)	44.60 to 2.34
<i>R</i> _{merge}	11.1 (84.3)*
<i>I</i> / σI	17.5 (1.9)
Completeness (%)	100.0 (100.0)
Redundancy	6.0 (5.8)
Refinement	
Resolution (Å)	44.60-2.34 (2.36-2.34)
No. reflections	55,808 (1,372)
<i>R</i> _{work} / <i>R</i> _{free}	21.2/25.4 (26.0/31.2)
No. atoms**	
Protein	7,537
GTP γ S-Mg ²⁺	99
Water	249
<i>B</i> -factors***	
Protein	44.7
GTP γ S-Mg ²⁺	30.4
Water	17.6
R.m.s. deviations	
Bond lengths (Å)	0.011
Bond angles (°)	1.249

*Values in parentheses are for the highest-resolution shell.

**Residues not assigned in molecule A: 30 to 31, 381 to 383, and 205-210; residues not assigned in molecule B: 97 to 128 and 153 to 160 in addition to all of those not assigned in molecule A; residues not assigned in molecule C: 65 to 72, 91 to 133, 145 to 157, and 204 to 212 in addition to all of those not assigned in molecule A.

***Assymmetric unit contained three protein monomers. The B-factors for proteins in molecules A, B, and C were 35.2, 44.9, and 56.3, respectively.

Table S2. GTP-binding rates for wild-type and mutant G protein α subunits. Mutations in areas of interest for nucleotide exchange were introduced by site-directed mutagenesis. GTP γ S binding rates were measured by intrinsic fluorescence with purified G protein α subunit (400 nM) and GTP γ S (2 μ M). Rates were measured at 24°C for AtGPA1 and 30°C for G α_{i1} , and are reported as min⁻¹.

Protein backbone	Mutation(s)	Location of mutation	Exchange rate
AtGPA1	Wild-type	N/A	3.1
	R39L	Interacts with α 5 helix	2.9
	V160L	Near GTP γ S/Domain interface	5.1
	P161S	Near GTP γ S/Domain interface	3.4
	T164A	Near GTP γ S/Domain interface	3.5
	Y214F	Interacts with α 5 helix	3.7
	R352F	Salt bridge with α 4 helix, near GTP γ S	2.0
	T354C	Contacts GTP γ S	2.3
	D369K	α 5 helix	4.3
	Δ 203-208	Plant-specific insert between SwI and SwII	1.4
	G α_{i1} α D/ α E ¹	Interdomain interactions	ND*
	G α_q C-term ²	Receptor coupling	4.2
	G α_{i1} C-term ³	Receptor coupling	3.5
G α_{i1} linkers ⁴	Connect helical and Ras domains	2.1	
G α_{i1}	Wild-type	N/A	0.04
	K192A	Contacts α 5 helix	0.06
	D337K	α 5 helix	0.13
	GPA1 linkers	Connects helical and Ras domains	0.01

*Rate not reported because protein could not be expressed.

¹Residues 146 to 177 (α D- α E) from AtGPA1 were replaced with homologous residues from G α_{i1} .

²The six most C-terminal residues of AtGPA1 were replaced with homologous residues from G α_q .

³The six most C-terminal residues of AtGPA1 were replaced with homologous residues from G α_{i1} .

⁴AtGPA1 linkers (residues 63 to 67 and 189 to 196) were replaced with homologous residues from G α_{i1} .

Movie S1. Movie depicting domain motion in AtGPA1 generated from MD simulations. This movie was rendered from the third most frequent mode of motion for AtGPA1. Although the guanine nucleotide was not included in the MD simulation, it is pictured here for reference. This mode (and others not shown) illustrates domain disengagement, which would potentially provide an exit route for the guanine nucleotide.